Experimental study of the 2n-transfer reaction ^{138}Ba(^{18}O,^{16}O)^{140}Ba in the projectile energy range 61–67 MeV

A. Khaliel[1(a)], T. J. Mertzimekis[1], F. C. L. Crespi[2], G. Zagoraios[1], D. Papaioannou[1], N. Florea[3], A. Turturica[3], L. Stan[3] and N. Mărginean[3]

[1] *Department of Physics, National & Kapodistrian University of Athens - Zografou Campus, GR-15784, Athens, Greece*
[2] *Università degli Studi di Milano and INFN sez. Milano - Milano, Italy*
[3] *National Institute for Physics and Nuclear Engineering - Magurele, Romania*

Abstract – Two-neutron transfer reactions serve as an important tool for nuclear-structure studies in the neutron-rich part of the nuclear chart. In this paper, we report on the first experimental attempt to populate the excited states of ^{140}Ba employing the 2n-transfer reaction ^{138}Ba(^{18}O, ^{16}O)^{140}Ba. ^{140}Ba is highly important, as it is placed on the onset of octupole correlations and the lifetimes of its excited states are completely unknown, with the sole exception of the first 2^+ state. The experiment was carried out at the Horia Hulubei National Institute for Physics and Nuclear Engineering (IFIN–HH) in Magurele, Romania. Lower limits on the lifetimes of the ground state band up to the 8^+ state are reported. Furthermore, relative cross-sections regarding the 2n-transfer reaction with respect to the fusion and the total inelastic reaction channels have been deduced. Further investigation directions of the nuclear structure of ^{140}Ba are also discussed.

Introduction. – Multinucleon Transfer Reactions (MTR) are important tools for nuclear structure studies [1–3]. Especially for energies close to the Coulomb barrier, transfer-reaction cross-sections are a large fraction of the total reaction cross-section [3], thus leading to a significant population of excited states of the produced nuclei. It is under discussion that such reactions can offer a new pathway for the study of neutron-rich transuranium isotopes and superheavy elements [4], as their expected yields are comparable to the fusion reactions, while providing the advantage of offering a wide range of populated isotopes during the same experiment.

Two-neutron transfer reactions have been successfully used for populating the excited states of nuclei, which are moderately rich in neutrons [5]. Recently, the neutron-rich ^{144,146}Ba isotopes were studied experimentally in terms of their $B(E3)$ values [6,7] using radioactive beams and Coulomb excitation. The respective $B(E3)$ values, although featuring large uncertainties, were found to be significantly larger than any theoretical prediction. Thus, a

study of ^{140}Ba is important for establishing the onset of octupole correlations, as well as assessing the degree of collectivity in the barium isotopic chain as a function of the neutron number. In addition, the lifetimes of the lower-lying states of ^{140}Ba are unknown, with the sole exception of the first 2_1^+ state, as reported in [8].

Cross-section data, either absolute or relative, are important for estimating the degree of level populations of the reaction products. Experimental cross-section data are still scarce for such reactions, especially for barium. Barium is a material that oxidizes very quickly when exposed to air, thus making the manufacturing of a target quite challenging and a "difficult" nucleus to study using stable beams.

In this work, we report on the relative cross-sections of the 2n-transfer reaction ^{18}O+^{138}Ba → ^{16}O + ^{140}Ba with respect to the fusion evaporation reaction ^{18}O+^{138}Ba → ^{152}Gd+4n, as well as to the total inelastic channel. These ratios can serve as a reference point for the theoretical studies, *i.e.*, refining Optical Model Potentials, or further experimental studies using such reactions. Furthermore, lower limits on lifetimes of the observed ground-state
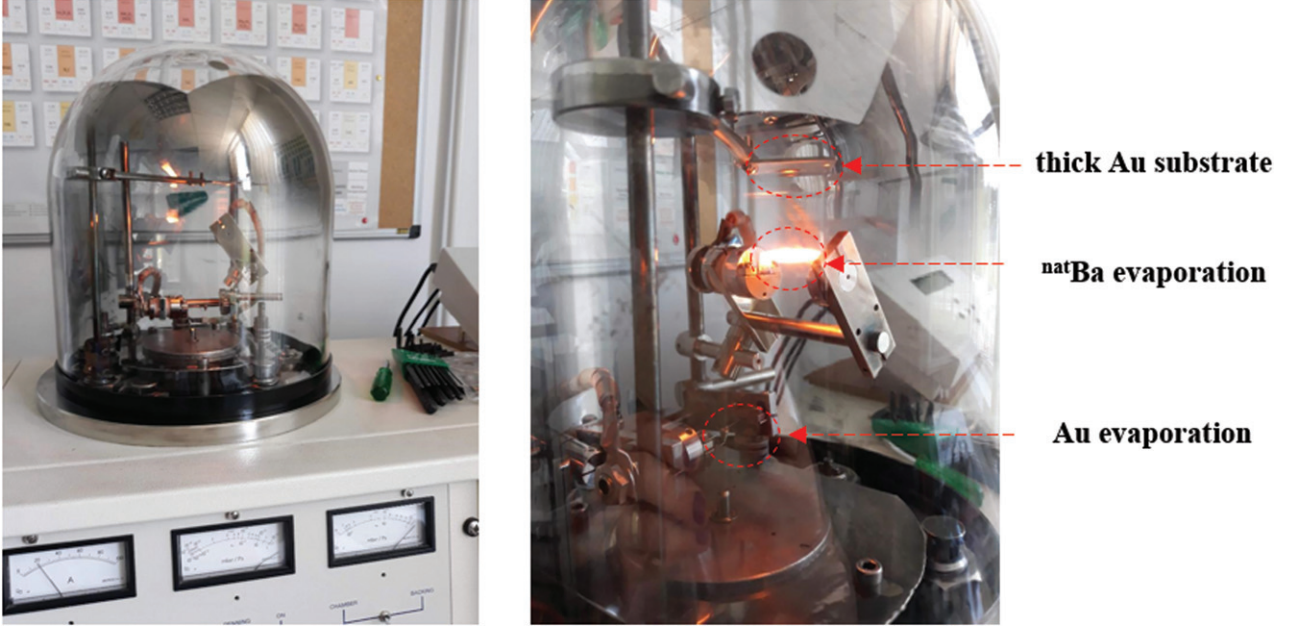
(a)E-mail: achalil@phys.uoa.gr

Fig. 1: The evaporator chamber (left) and a picture taken during the evaporation procedure (right).

band states are reported by taking into consideration the limitations of the Doppler Shift Attenuation Method (DSAM) [9,10] for the particular system.

Experimental details. –

Experimental setup. The experiment was carried out at the 9 MV Tandem Accelerator Laboratory at the Horia Holubei National Institute of Physics and Nuclear Engineering (IFIN–HH) in Magurele, Romania. Four projectile energies were studied near the Coulomb barrier of the reaction, namely 61, 63, 65 and 67 MeV. The subsequent γ decay was detected by the ROSPHERE array [11] loaded with 15 HPGe detectors.

Target manufacturing. The manufacturing of the ^{nat}Ba target in metallic form presents important difficulties, as it is a material that oxidizes extremely fast. Therefore, as illustrated in fig. 1, a gold-sandwiched ^{nat}Ba target was prepared in the Target Preparation Laboratory of IFIN–HH [12]. The target exhibits the following structure: Au $(4.88 \, \mathrm{mg \, cm^{-2}})/^{nat}$Ba $(2 \, \mathrm{mg \, cm^{-2}})/$Au $(0.5 \, \mathrm{mg \, cm^{-2}})$. The metallic ^{nat}Ba layer (abundance of ^{138}Ba = 71.7%) was obtained through the metalothermic reduction reaction of $BaCO_3$ with La metal powder as reducing agent. For this purpose about double the stoichiometric amount of La metal powder was thoroughly ground with the calculated amount of $BaCO_3$, in an agate mortar set. The resulted mixture was pressed into a pellet, which was inserted into a pinhole tantalum boat. Both ends of the boat were fixed to the high current electrodes of the Quorum technologies E6700 bench top evaporator device. The gold foil of $4.88 \, \mathrm{mg \, cm^{-2}}$ thickness, prepared in advance by rolling, was glued to the target frame and placed 4 cm above the tantalum boat in the evaporator.

After a high vacuum of 3.5×10^{-5} mbar was reached, a low current was applied through the tantalum boat to degassing of CO_2 resulted from the thermal decomposition of $BaCO_3$. Therefore, the current through the tantalum boat was slightly increased until the reduction temperature was reached. The evaporation process was carried out until the desired thickness was obtained. The obtained ^{nat}Ba layer was covered with a thin gold layer of $0.5 \, \mathrm{mg \, cm^{-2}}$ without breaking the vacuum, to protect the metallic ^{nat}Ba against oxidation. This deposition was made with a tungsten basket, fixed at 9 cm distance above the substrate.

The determination of the thick gold backing's thickness was done by weighing, while the other two layers were determined by calculating the thickness from the initial amount of the substance used.

Analysis and results. –

Lifetimes. Lower limits on lifetimes of the states up to 8^+ in the ground-state band [13], corresponding to the observed transitions can be set, by taking into account the limitation of the Doppler Shift Attenuation Method (DSAM). In fig. 2(a), the two overlapping transitions of energies 528 and 530 keV are shown, depopulating the 4^+ and 6^+ states of the ground-state band. As it can be seen for the spectra recorded in the backward (143°) and forward ring (37°), no visible lineshapes can be distinguished. The same holds for fig. 2(b), where the transition of 808 keV is depopulating the 8^+, also in the ground-state band.

The maximum recoil velocity in the particular reaction mechanism is 2% the speed of light. At such recoil velocities, the range of lifetimes that can be measured with DSAM should be lower than approximately 1 ps [9,14–16].
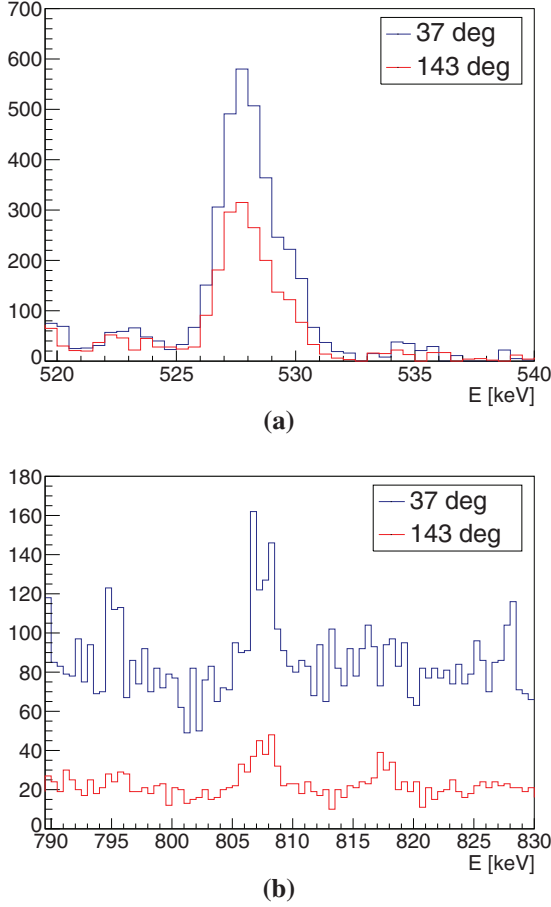
(a)

(b)

Fig. 2: Backward (143°) and forward (37°) spectra for (a) the 528 and 530 keV overlapping transitions, and (b) the 808 keV transition. The spectra show no backward-forward lineshapes.
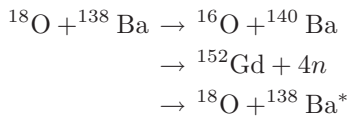
The present limit is established in terms of the range of lifetimes that the particular method can be applied, and not the sensitivity of the experimental setup.

Relative cross-sections. The cross-section of a reaction can be estimated by the relation

$$\sigma = \frac{N_R}{\Phi N_t}, \tag{1}$$

where N_R is the number of occurring reactions, N_t is the number of target nuclei that the beam interacts with, and Φ is the incident flux of projectiles.

The reactions

$$^{18}\text{O} + ^{138}\text{Ba} \rightarrow ^{16}\text{O} + ^{140}\text{Ba}$$
$$\rightarrow ^{152}\text{Gd} + 4n$$
$$\rightarrow ^{18}\text{O} + ^{138}\text{Ba}^*$$

stem from the same entry channel and occur inside the barium foil. In general, the relative cross-section for two different exit channels α, β can be estimated by
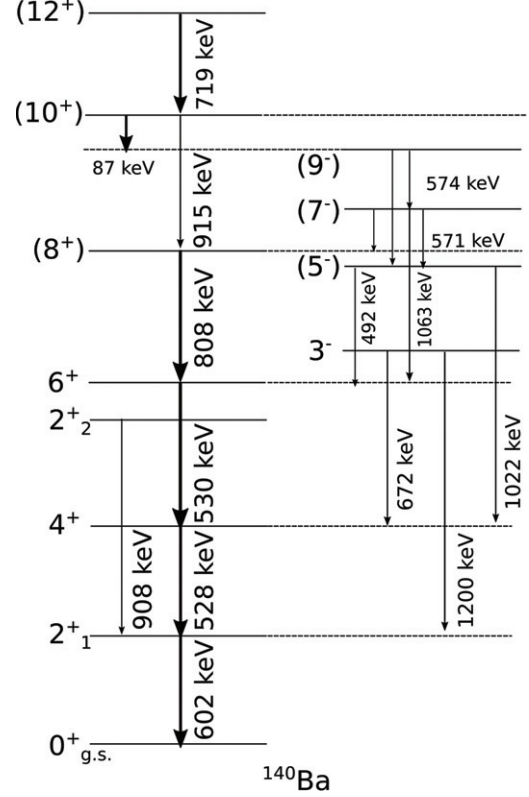
$$\sigma_R = \frac{N_R(\alpha)}{N_R(\beta)}, \tag{2}$$

Fig. 3: Partial level scheme of ^{140}Ba, showing the ground-state band and a side band [13]. The alternating parity of the states of two bands is a hint for significant octupole correlations.

i.e., by determining the ratios of the corresponding number of reactions.

In the present case, the number of reactions can be deduced by measuring all observed photopeaks feeding the ground state of the produced nuclei for the two above exit channels, and then correcting with the full absolute efficiency of the ROSPHERE array:

$$N_R = \frac{A}{\epsilon_{abs}}, \tag{3}$$

where A is the area of the photopeak and ϵ_{abs} is the absolute efficiency.

For the 2n-reaction ^{18}O + ^{138}Ba $\rightarrow$ ^{16}O + ^{140}Ba, only the $E_\gamma = 602$ keV transition was observed (see fig. 3), while for the ^{18}O + ^{138}Ba $\rightarrow$ ^{152}Gd + 4n reaction, only the transition with $E_\gamma = 344$ keV was recorded in the data. Also, for the total inelastic channel, the transition $E_\gamma = 1436$ keV was observed. A projection spectrum of the full γ-γ matrix is shown in fig. 4, with the peaks of interest marked.

By extracting the ratios, and taking into account the energy loss inside the barium foil of the target (table 1), the results for the relative cross-sections of the 2n-transfer reaction ^{18}O + ^{138}Ba $\rightarrow$ ^{16}O + ^{140}Ba with respect to the fusion-evaporation counterpart ^{18}O + ^{138}Ba $\rightarrow$ ^{152}Gd + 4n and with respect to the total inelastic channel are shown in fig. 5 as a function of energy in the laboratory system.
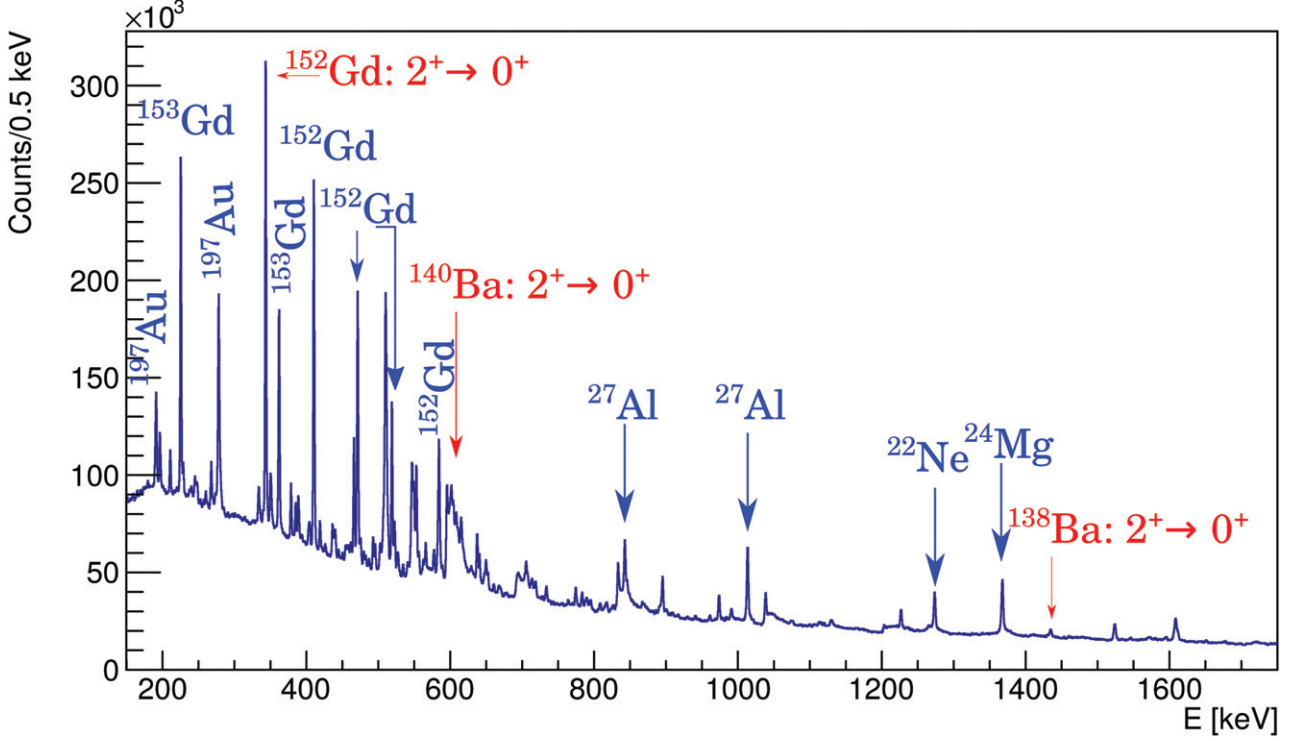
Fig. 4: Total projection spectrum from the γ-γ matrix acquired using the ROSPHERE array. Transitions in barium isotopes are marked, as well as several from the fusion-evaporation channels. A few contaminant peaks are also indicated.

Table 1: Experimental results and theoretical calculations. From left to right column: E_b is the beam energy; E_{Ba} is the incident energy of at the front of the Barium foil, by taking into consideration the beam energy loss inside the front Au foil; ΔE_{Ba} is the total energy loss in the barium foil; E_{eff} is the effective energy at the middle of the barium foil; σ_R^{fus} is the ratio of the 2n-transfer reaction cross-section over the cross-section of the fusion-evaporation channel (see eq. (2)); σ_R^{inel} is the ratio of the 2n-transfer reaction cross-section over the total inelastic cross-section; σ_{Gd} and σ_{Ba} are normalized cross-sections (see text for details); σ_{PACE} and $\sigma_{GRAZING}$ are results of `PACE4` and `GRAZING_9` calculations for the $^{18}O + ^{138}Ba \rightarrow ^{152}Gd + 4n$ and $^{18}O + ^{138}Ba \rightarrow ^{16}O + ^{140}Ba$ reactions, respectively. All values are in the laboratory system.

| E_b (MeV)	E_{Ba} (MeV)	ΔE_{Ba} (MeV)	E_{eff} (MeV)	σ_R^{fus}	σ_R^{inel}	σ_{Gd} (mb)	σ_{Ba} (mb)	σ_{PACE4} (mb)	$\sigma_{GRAZING}$ (mb)
61	60.04	4.91	57.59	0.3 ± 0.1	0.7 ± 0.4	0.43 ± 0.01	0.11 ± 0.06	–	0.1112
63	62.05	4.83	59.64	0.12 ± 0.01	0.8 ± 0.1	2.46 ± 0.01	0.29 ± 0.04	0.00178	0.33087
65	64.06	4.75	61.69	0.107 ± 0.006	1.8 ± 0.1	8.02 ± 0.04	0.86 ± 0.06	0.847	0.63257
67	66.07	4.68	63.73	0.06 ± 0.01	2.0 ± 0.5	23.4 ± 0.1	1.5 ± 0.3	23.4	0.89368

Cross-section predictions. – In order to further investigate the experimental values of the relative cross-sections measured in the present work, theoretical calculations have been performed using the `GRAZING_9` [17] and `PACE4` [18] codes.

The former uses Winther's grazing model [17], which has been proven successful for the description of one- or two-nucleon transfer reactions [19]. Calculations performed with the `GRAZING_9` code use a semi-classical approach developed in ref. [20]. For a small number of nucleon transfers (up to 6–8 neutrons) and for nuclei close to the magic shell closures, the particular model describes

experimental data very well; however, it tends to slightly underestimate the data for large numbers of nucleons (see discussion in [21]).

On the other hand, the `PACE4` code is the latest version of a modified JULIAN code [22] and uses the Bass model [23], which was derived by using a geometric interpretation of available experimental data combined with a Monte Carlo approach to determine the decay of the compound system in the framework of Hauser-Feshbach formalism [24]. As stated in ref. [19], the Bass model potential provides an overall excellent description for the fusion cross-sections at energies starting from the Coulomb
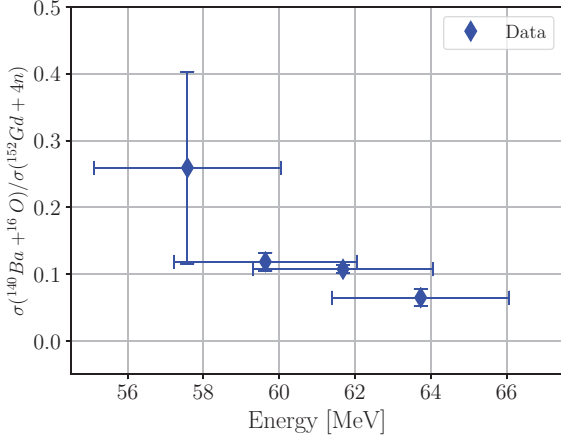
(a)
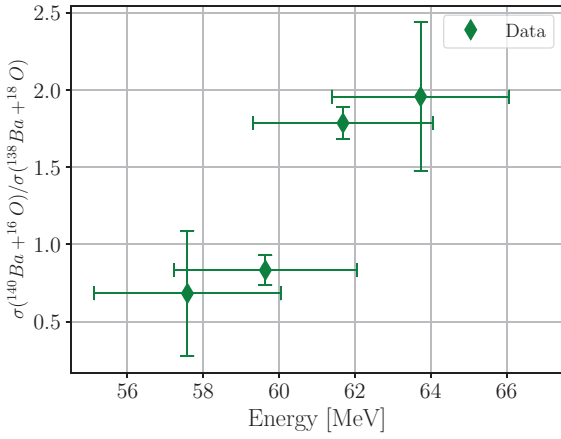
(b)

Fig. 5: Relative cross-section of the two neutron-transfer reaction ^{18}O + ^{138}Ba → ^{16}O + ^{140}Ba with respect to the fusion evaporation reaction ^{18}O + ^{138}Ba → ^{152}Gd + 4n (a) and the ratio with respect to the total inelastic channel ^{18}O + ^{138}Ba → ^{16}O + ^{138}Ba* (b).

barrier and above. However, experimental evidence shows that the particular model significantly underestimates the cross-section data below the Coulomb barrier [19].

All calculations have been performed using the default parameters each code employs. Figure 6 shows the results of the calculations: fig. 6(a) includes cross-section calculations with PACE4 (solid circles), while fig. 6(b) contains calculated cross-sections with GRAZING_9 (solid squares). PACE4 could not produce a value at the lowest energy (E_{eff} = 57.6 MeV), as was expected, since this value is far below the barrier. The experimental absolute yield for the fusion-evaporation channel is shown in fig. 6 (solid diamonds). All data points have been normalized with a single numerical factor. That factor was estimated by scaling the experimental point at the energy nearest to the barrier (E_{eff} = 63.7 MeV) with the respective value calculated with PACE4 (see overlapping points in fig. 6(a)).

Calculations with GRAZING_9 are shown in fig. 6(b) (solid squares). In the same graph, experimental data of the 2n-transfer reaction ^{18}O + ^{138}Ba → ^{16}O + ^{140}Ba are
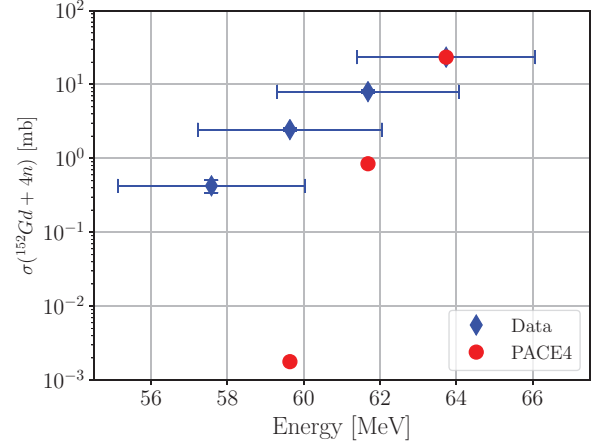
(a)
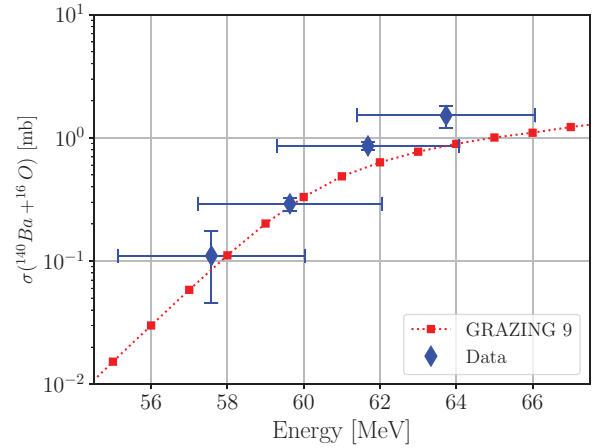
(b)

Fig. 6: (a) Normalized cross-sections of the fusion-evaporation channel after normalization to PACE4 calculations (see text). Vertical error bars are smaller than the symbol size. (b) Deduced cross-sections for the 2n-transfer channel (solid diamonds) after taking into account the results from panel (a), together with GRAZING_9 calculations (solid squares). No scaling is involved in any of the data sets in panel (b). The dotted line is to guide the eye. Scales of y-axes in (a) and (b) are different.

shown. These data have been extracted from the ratio in fig. 5 taking into account the scaled cross-sections of the fusion-evaporation channel, as described earlier. No further scaling is involved.

Discussion and future investigations. – Within the present framework, a study of the nucleus ^{140}Ba by using the 2n-transfer reaction ^{18}O + ^{138}Ba → ^{16}O + ^{140}Ba, has been performed. By considering the kinematics of the reaction studied and the limitation of DSAM, lower limits on the lifetimes of 3 states of the ground state band have been set over 1 ps. Of course, further studies are necessary in order to further constrain the above limit. The present results also set the path for using a different technique for the measurement of the particular lifetimes, such as the plunger technique or the fast-timing technique. For direct

measurement of the reduced transition probabilities, especially for the $B(E3)$ corresponding to the first 3^- state, the use of radioactive beams and Coulomb excitation technique can override a lot of issues, such as possible target contamination and the level population strength.

The relative cross-sections between the 2n-transfer reaction $^{18}\text{O} + ^{138}\text{Ba} \rightarrow ^{16}\text{O} + ^{140}\text{Ba}$ and the competing fusion-evaporation reaction $^{18}\text{O} + ^{138}\text{Ba} \rightarrow ^{152}\text{Gd} + 4n$ have been deduced by taking into account the relative yield of the two observed transitions feeding the ground state of the two produced nuclei. The relative cross-section behavior seems to follow a reducing pattern with respect to beam energy, showing that the fusion-evaporation channel becomes stronger faster, as the Coulomb barrier is approached. This behavior is rather expected given the fact that the reactions occur in the pure-tunneling energy range. In addition, the relative cross-sections of the reaction $^{18}\text{O} + ^{138}\text{Ba} \rightarrow ^{16}\text{O} + ^{140}\text{Ba}$ and the total inelastic channel are presented. The inelastic channel is a competing reaction channel, for which, as can be seen from fig. 5(b), the respective cross-section values are of the same order of magnitude within the studied energy range. The behavior of these cross-sections follows an increasing pattern, indicating that the 2n-transfer reaction shows a stronger increase as the energy increases towards the Coulomb barrier.

Absolute cross-sections deduced with this method, taking advantage of the ratios of cross-sections, may be lower than their actual values, as some transitions feeding the ground state may not be observed in the spectra, resulting in missing strength in the overall estimation. In addition, the ^{152}Gd decay features $E0$ transitions directly to the ground state. It is very hard to observe such transitions in the γ-spectrum, despite their contribution to the total number of produced nuclei. While this can be usually treated as a weak effect, it cannot be assumed with certainty.

Calculations with the theoretical codes `PACE4` and `GRAZING_9` have been performed to provide a comparison with experimental data produced in the present work. The scaling of the experimental data to the `PACE4` result at the maximum energy, almost identical to the energy of the barrier, can be trusted to produce absolute cross-sections for the absolute cross-sections in the fusion-evaporation channels. This becomes evident when the deduced cross-sections for the studied 2n-transfer reaction are further compared to `GRAZING_9` calculations. These calculations can also estimate the ground-state production of ^{140}Ba, which cannot be deduced from the γ-ray spectrum [17,25]. However, the calculated distribution of the total kinetic energy loss following the transfer reaction suggests that the cross-section for producing reaction products directly in their ground state is at least one order of magnitude lower than producing them at higher excitation energies at the energy region of this work. Thus, in the present analysis, the ground-state production of ^{140}Ba has been ignored.

There is a very good agreement between experimental data and theory, both in trend and in magnitude. The two lowest energy points are effectively the same within the experimental uncertainty, while the discrepancy between the rest is of the order of 20%. It has to be stressed again that this comparison involves no other scaling than the one used for the fusion-evaporation channel. It would be interesting also to check this method in more detail for energies near and above the barrier in the future, especially for neighboring nuclei in this mass regime.

In conclusion, the results provide useful information for the specific case study, for both the experimental cross-sections, as well as the validity of theoretical models at energies near the barrier. 2n-transfer reactions are a very useful tool to study unstable, moderately neutron-rich nuclei. To this end, the knowledge of the 2n-transfer–to–fusion cross-section ratio can be extremely useful, for example, for reducing the fusion background, especially in nuclear structure studies. In addition, cross-section ratios can help in constraining the optical model potential phenomenological parameters, for the better understanding of systems involving heavy-ion reactions. Such experimental data in the region around ^{140}Ba are very scarce, but also very important for studies trying to extend our knowledge on more exotic species towards the neutron dripline.

$$* * *$$

REFERENCES

[1] Szilner S., Ur C. A., Corradi L., Mărginean N., Pollarolo G., Stefanini A. M., Beghini S., Behera B. R., Fioretto E., Gadea A., Guiot B., Latina A., Mason P., Montagnoli G., Scarlassara F., Trotta M., Angelis G. d., Vedova F. D., Farnea E., Haas F., Lenzi S., Lunardi S., Mărginean R., Menegazzo R., Napoli D. R., Nespolo M., Pokrovsky I. V., Recchia F., Romoli M., Salsac M.-D., Soić N. and Valiente-Dobón J. J., *Phys. Rev. C*, **76** (2007) 024604.
[2] Zagrebaev V. and Greiner W., *Phys. Rev. Lett.*, **101** (2008) 122701.
[3] Corradi L., Pollarolo G. and Szilner S., *J. Phys. G: Nucl. Part. Phys.*, **36** (2009) 113101.
[4] Heinz S., *J. Phys.: Conf. Ser.*, **1014** (2018) 012005.
[5] Leoni S., Fornal B., Mărginean N., Sferrazza M., Tsunoda Y., Otsuka T., Bocchi G., Crespi F. C. L., Bracco A., Aydin S., Boromiza M., Bucurescu D., Cieplicka-Oryǹczak N., Costache C., Călinescu S., Florea N., Ghiţă D. G., Glodariu T., Ionescu A., Iskra L., Krzysiek M., Mărginean R., Mihai C.,

MIHAI R. E., MITU A., NEGREȚ A., NIȚĂ C. R., OLĂCEL A., OPREA A., PASCU S., PETKOV P., PETRONE C., PORZIO G., ȘERBAN A., SOTTY C., STAN L., ȘTIRU I., STROE L., ȘUVĂILĂ R., TOMA S., TURTURICĂ A., UJENIUC S. and UR C. A., *Phys. Rev. Lett.*, **118** (2017) 162502.

[6] BUCHER B., ZHU S., WU C. Y., JANSSENS R. V. F., CLINE D., HAYES A. B., ALBERS M., AYANGEAKAA A. D., BUTLER P. A., CAMPBELL C. M., CARPENTER M. P., CHIARA C. J., CLARK J. A., CRAWFORD H. L., CROMAZ M., DAVID H. M., DICKERSON C., GREGOR E. T., HARKER J., HOFFMAN C. R., KAY B. P., KONDEV F. G., KORICHI A., LAURITSEN T., MACCHIAVELLI A. O., PARDO R. C., RICHARD A., RILEY M. A., SAVARD G., SCHECK M., SEWERYNIAK D., SMITH M. K., VONDRASEK R. and WIENS A., *Phys. Rev. Lett.*, **116** (2016) 112503.

[7] BUCHER B., ZHU S., WU C. Y., JANSSENS R. V. F., BERNARD R. N., ROBLEDO L. M., RODRÍGUEZ T. R., CLINE D., HAYES A. B., AYANGEAKAA A. D., BUCKNER M. Q., CAMPBELL C. M., CARPENTER M. P., CLARK J. A., CRAWFORD H. L., DAVID H. M., DICKERSON C., HARKER J., HOFFMAN C. R., KAY B. P., KONDEV F. G., LAURITSEN T., MACCHIAVELLI A. O., PARDO R. C., SAVARD G., SEWERYNIAK D. and VONDRASEK R., *Phys. Rev. Lett.*, **118** (2017) 152504.

[8] BAUER C., BEHRENS T., BILDSTEIN V., BLAZHEV A., BRUYNEEL B., BUTTERWORTH J., CLÉMENT E., COQUARD L., EGIDO J. L., EKSTRÖM A., FITZPATRICK C. R., FRANSEN C., GERNHÄUSER R., HABS D., HESS H., LESKE J., KRÖLL T., KRÜCKEN R., LUTTER R., MARLEY P., MÖLLER T., OTSUKA T., PATRONIS N., PETTS A., PIETRALLA N., RODRÍGUEZ T. R., SHIMIZU N., STAHL C., STEFANESCU I., STORA T., THIROLF P. G., VOULOT D., VAN DE WALLE J., WARR N., WENANDER F. and WIENS A., *Phys. Rev. C*, **86** (2012) 034310.

[9] ALEXANDER T. K. and FORSTER J. S., *Lifetime Measurements of Excited Nuclear Levels by Doppler-Shift Methods* (Springer US, Boston, MA) 1978, pp. 197–331.

[10] PETKOV P., TONEV D., GABLESKE J., DEWALD A. and VON BRENTANO P., *Nucl. Instrum. Methods Phys. Res. Sect. A: Accelerators, Spectrometers, Detectors and Associated Equipment*, **437** (1999) 274.

[11] BUCURESCU D., CTA-DANIL I., CIOCAN G., COSTACHE C., DELEANU D., DIMA R., FILIPESCU D., FLOREA N., GHI D., GLODARIU T., IVACU M., LIC R., MRGINEAN N., MRGINEAN R., MIHAI C., NEGRET A., NI C., OLCEL A., PASCU S., SAVA T., STROE L., ERBAN A., UVIL R., TOMA S., ZAMFIR N., CTA-DANIL G., GHEORGHE I., MITU I., SULIMAN G., UR C., BRAUNROTH T., DEWALD A., FRANSEN C., BRUCE A., PODOLY Z., REGAN P. and ROBERTS O., *Nucl. Instrum. Methods Phys. Res. Sect. A: Accelerators, Spectrometers, Detectors and Associated Equipment*, **837** (2016) 1.

[12] FLOREA N. M., STROE L., MĂRGINEAN R., GHIȚĂ D. G., BUCURESCU D., BADEA M., COSTACHE C., LICĂ R., MĂRGINEAN N., MIHAI C., MOȘU D. V., NIȚĂ C. R., PASCU S. and SAVA T., *J. Radioanal. Nucl. Chem.*, **305** (2015) 707.

[13] The Evaluated Nuclear Structure Data File (ENSDF), https://www.nndc.bnl.gov/ensdf/ (accessed 2019).

[14] PETKOV P., DEWALD A. and VON BRENTANO P., *Nucl. Instrum. Methods Phys. Res. Sect. A: Accel., Spectrom., Detect. Assoc. Equip.*, **560** (2006) 564.

[15] MIHAI C., PASTERNAK A. A., FILIPESCU D., IVAȘCU M., BUCURESCU D., CĂTA DANIL G., CĂTA DANIL I., DELEANU D., GHIȚĂ D., GLODARIU T., LOBACH Y. N., MĂRGINEAN N., MĂRGINEAN R., NEGRET A., PASCU S., SAVA T., STROE L., SULIMAN G. and ZAMFIR N. V., *Phys. Rev. C*, **81** (2010) 034314.

[16] PETKOV P., *AIP Adv.*, **8** (2018) 075305.

[17] WINTHER A., *Nucl. Phys. A*, **572** (1994) 191.

[18] GAVRON A., *Phys. Rev. C*, **21** (1980) 230.

[19] REISDORF W., *J. Phys. G: Nucl. Part. Phys.*, **20** (1994) 1297.

[20] WENDT K., AHMAD S. A., EKSTRÖM C., KLEMPT W., NEUGART R. and OTTEN E. W., *Z. Phys. A At. Nucl.*, **329** (1988) 407.

[21] SAMARIN V. V., *Bull. Russ. Acad. Sci.: Physics*, **77** (2013) 820.

[22] HILLMAN M. and EYAL Y., *Phys. Rev. C*, **21** (1980) 230.

[23] BASS R., *Phys. Rev. Lett.*, **39** (1977) 265.

[24] HAUSER W. and FESHBACH H., *Phys. Rev.*, **87** (1952) 366.

[25] WINTHER A., *GRAZING_9, A Fortran program for estimating reactions in collision between heavy nuclei*, http://personalpages.to.infn.it/~nanni/grazing/.